TI Designs

Voltage, Current, and Temperature Monitoring for Solar Module Level Power Electronics

Description

This verified reference design provides an overview on how to implement a solar module level monitoring and communication subsystem. This TI Design addresses the key need of a highly cost-optimized monitoring and communication subsystem for solar module level power electronics (MLPE). This design showcases a highly integrated solution for accurate voltage, current, and temperature monitoring along with ZigBee® communication using the CC2538 to enable solar module level monitoring.

Features

- <2% Error Voltage Measurement
- <2% Error Current Measurement
- CC2538 M3 SoC for ZigBee Communication
- PCB Based Antenna With Simplified Filtering Circuitry

Applications

- Solar Energy Monitoring and Communications

Resources

TIDA-00640	Design Folder
CC2538	Product Folder
LM5017	Product Folder
TLV342A	Product Folder

TI E2E™ Community — ASK Our E2E Experts

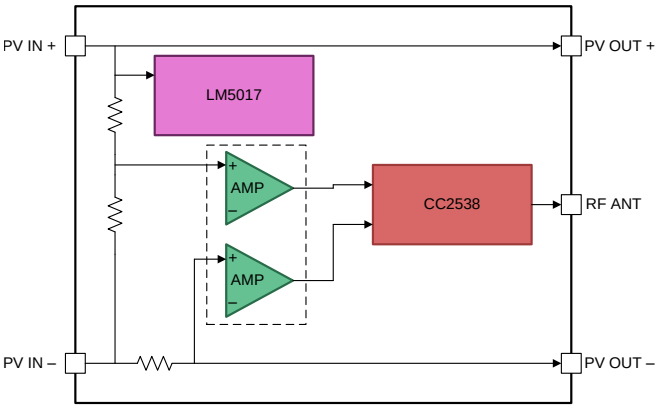

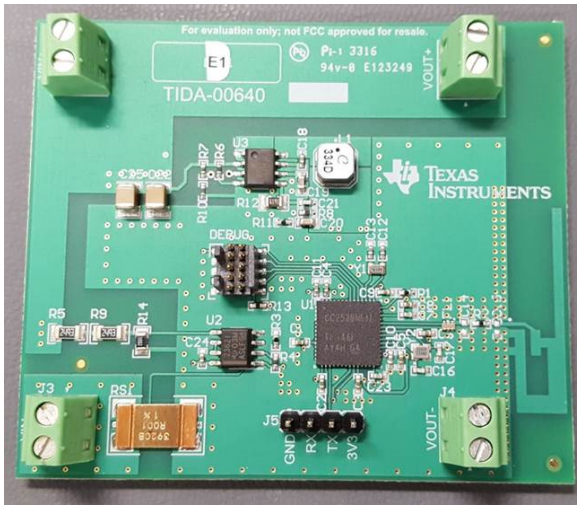

An IMPORTANT NOTICE at the end of this TI reference design addresses authorized use, intellectual property matters and other important disclaimers and information.

1 System Overview

1.1 System Description

Module level power electronics (MLPEs) provide a very granular method of optimizing a solar system. Moving the maximum power point tracking (MPPT) or other power management services to the module reduces the cost overhead on a system and enables a higher total system power output. However, it removes some of the capability of monitoring string degradation because every module appears to perform optimally to an outside observer. The addition of integrated power measurement at each MLPE enables several additional features:

- Array performance metrics to evaluate instillation return on investment
- Mesh based power point tracking more efficient power conversion
- Module degradation information due to aging or soiling
- Module mismatch and instillation issue analysis

The TIDA-00640 integrates the voltage, current, and temperature measurement into a single system that is able to be powered by the module itself and wireless communicate the data back to a central point through a number of wireless standards. This TI Design enables quick integration of the measurement and wireless technology with MPLEs to make a full distributed power conversion system.

1.2 Key System Specifications

Table 1. Key System Specifications

PARAMETER	SPECIFICATIONS	DETAILS
Voltage Input	10- to 90-V input voltage support for modern HV modules	Section 2.1
Sensor type	Shunt resistor	Section 2.2
Current measurement accuracy	<2% calibrated and uncalibrated error full scale	Section 4.2
Voltage measurement accuracy	<2% calibrated and <2.5% uncalibrated error full scale	Section 4.1
Temperature measurement	±5°C	Section 2.6
Wireless functionality	1 minute of no motion detected	Section 2.5

1.3 Block Diagram

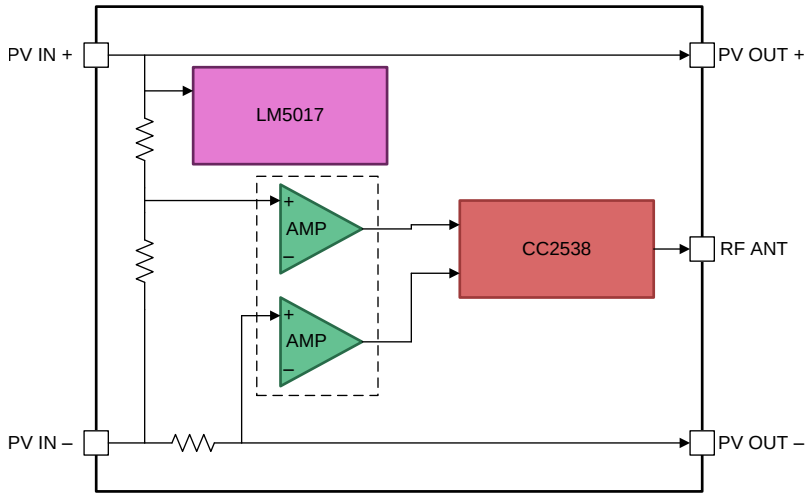

Figure 1. TIDA-00640 System Block Diagram

1.4 Highlighted Products

1.4.1 CC2538

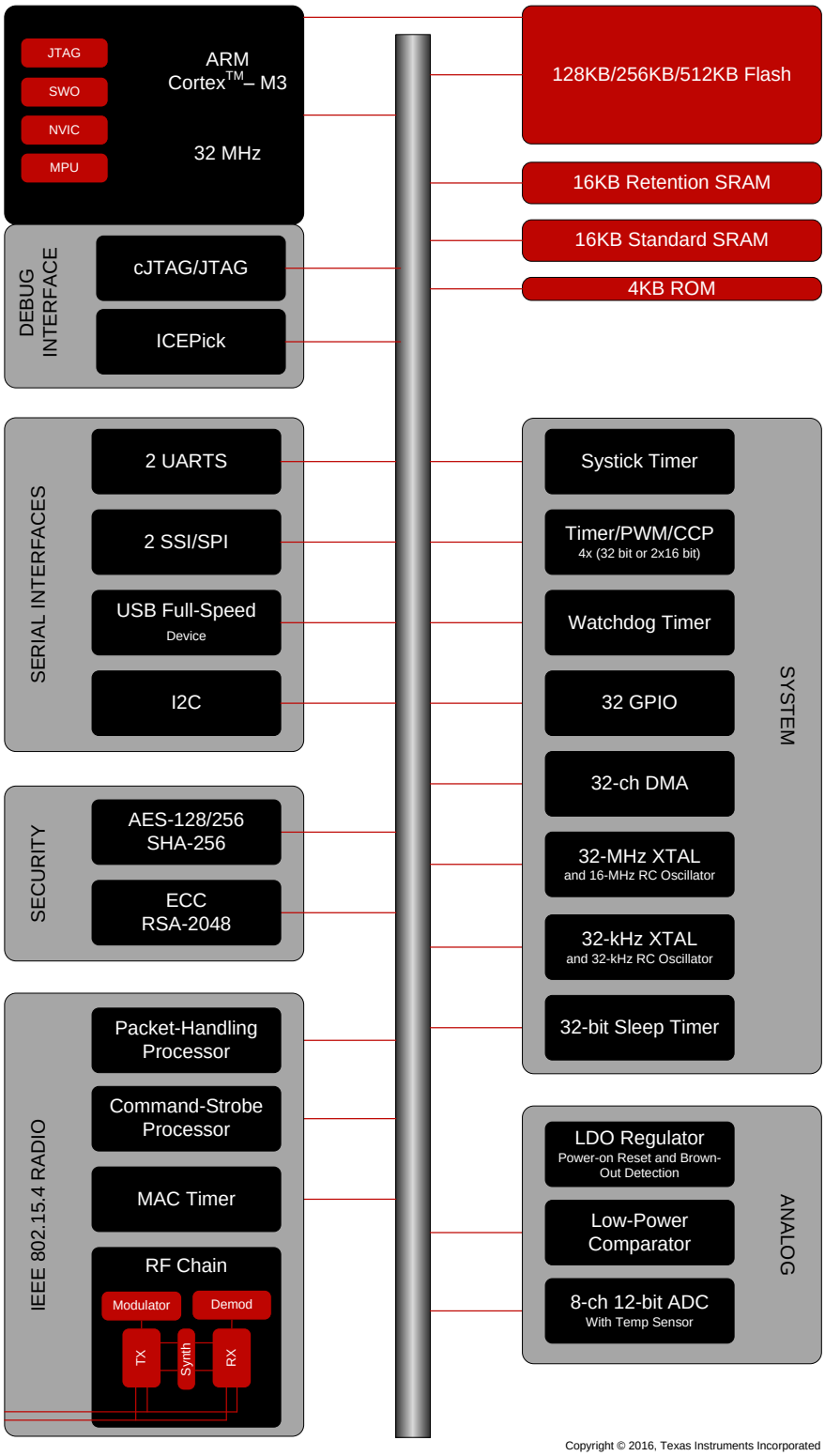

Figure 2. CC2538 Device Block Diagram

- Microcontroller
  - Powerful ARM® Cortex®-M3 with Code Prefetch
  - Up to 32-MHz clock speed
  - 512KB, 256KB, or 128KB of in-system-programmable flash
  - Supports on-chip over-the-air upgrade (OTA)
  - Supports dual ZigBee application profiles
  - Up to 32KB of RAM (16KB with retention in all power modes)
  - cJTAG and JTAG debugging
- RF
  - 2.4-GHz IEEE 802.15.4 compliant RF transceiver
  - Excellent receiver sensitivity of –97 dBm
  - Robustness to interference with ACR of 44 dB
  - Programmable output power up to 7 dBm
- Security hardware acceleration
  - Future proof AES-128/256, SHA2 hardware encryption engine
  - Optional: ECC-128/256, RSA hardware acceleration engine for secure key exchange
  - Radio command strobe processor and packet handling processor for low-level MAC Functionality
- Low power
  - Active-Mode RX (CPU Idle): 20 mA
  - Active-Mode TX at 0 dBm (CPU Idle): 24 mA
  - Power Mode 1 (4-µs Wake-Up, 32-KB RAM retention, full register retention): 0.6 mA
  - Power Mode 2 (sleep timer running, 16-KB RAM retention, configuration register retention): 1.3 µA
  - Power Mode 3 (external interrupts, 16-KB RAM retention, configuration register retention): 0.4 µA
  - Wide supply-voltage range (2 to 3.6 V)
- Peripherals
  - µDMA
  - 4× general-purpose timers (each 32-bit or 2× 16-bit)
  - 32-bit 32-kHz sleep timer
  - 12-bit ADC with eight channels and configurable resolution
  - Battery monitor and temperature sensor
  - USB 2.0 full-speed device (12 Mbps)
  - 2× SPI
  - 2× UART
  - I^2C
  - 32 general-purpose I/O pins (28 × 4 mA, 4 × 20 mA)
  - Watchdog timer
- Layout
  - 8-mm × 8-mm QFN56 package
  - Robust device for industrial operation up to 125°C
  - Few external components
  - Only a single crystal needed for asynchronous networks

- Development tools
  - CC2538 development kit
  - Reference design certified under FCC and ETSI regulations
  - Full software support for Contiki/6LoWPAN, smart grid, lighting, and ZigBee home automation with sample applications and reference designs available
  - Code Composer Studio™
  - IAR Embedded Workbench® for ARM
  - SmartRF™ Studio
  - SmartRF Flash Programmer

1.4.2 LM5017

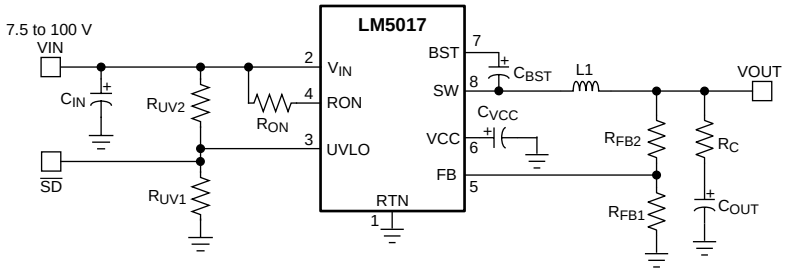

Figure 3. LM5017 Typical Application

- Wide 7.5- to 100-V input range
- Integrated 100-V high-side, and low-side switches
- No Schottky required
- Constant on-time control
- No loop compensation required
- Ultra-fast transient response
- Nearly constant operating frequency
- Intelligent peak current limit
- Adjustable output voltage from 1.225 V
- Precision 2% feedback reference
- Frequency adjustable to 1 MHz
- Adjustable undervoltage lockout (UVLO)
- Remote shutdown
- Thermal shutdown

1.4.3 TLV342A

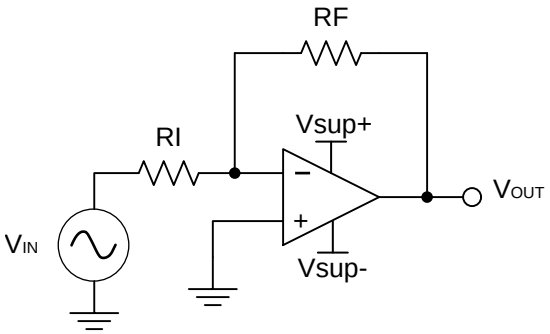

Figure 4. TLV342A Typical Application

- 1.8- and 5-V performance
- Low offset (A Grade)
  - 1.25 mV maximum (25°C)
  - 1.7 mV maximum (–40°C to 125°C)
- Rail-to-rail output swing
- Wide common-mode input voltage range: –0.2 V to (V+ – 0.5 V)
- Input bias current: 1 pA (typical)
- Input offset voltage: 0.3 mV (typical)
- Low supply current: 70 µA/channel
- Low shutdown current: 10 pA (typical) per channel
- Gain bandwidth: 2.3 MHz (typical)
- Slew rate: 0.9 V/µs (typical)
- Turnon time from shutdown: 5 µs (typical)
- Input referred voltage noise (at 10 kHz): 20 nV/√Hz
- ESD protection exceeds JESD 22
  - 2000-V human-body model (HBM)
  - 750-V charged-device model (CDM)

2 System Design Theory

2.1 Power Input

The intent of this TI Design is to be fully powered by the solar module from which it is measuring power. Modern solar modules are increasing in voltage in order to produce a higher power output without the need to scale the current passing capabilities. At the time writing, common solar modules have a nominal voltage rating in the mid 70 V and power output capabilities in excess of 300 W. These values are only expected to increase as the solar cell technology advances.

To satisfy the growing input voltage requirements of solar cells, the TIDA-00640 is specified with a very wide input voltage of up to 90 V. This is accomplished with the LM5017 step-down regulator, which is capable of handling input voltages from 7.5 to 100 V. This range is very well suited to the dynamic nature of PV modules, which can have wide voltage output swings dependent of current illuminance and temperature. It enables very high step-down voltages, from the 90-V input, to the 3.3 V required for the VCC in this TI Design.

The LM5017 contains internal switches with switch current handling of 600 mA. The total current draw of the system at its VCC rail is expected to be < 200 mA, even when transmitting, which is well within the output range of the LM5017 even at lower efficiency operation points. Being this far below the max operating current will also keep any self-heating to a minimum.

To keep the system cost and complexity low for the TIDA-00640, a type 1 configuration from the LM5017 datasheet was chosen. Find additional information on designing power stages using this configuration in the LM5017 datasheet[1]. If a more stable VCC is required, then a type 3 configuration can be implemented, but does add additional components to the power stage. This could be desirable to generate a more stable V_{REF} for the analog sensing circuitry.

A final consideration in the power stage is the type of components selected. In most switch mode power stages, a large electrolytic capacitor is used on the input to reduce input voltage ripple. This is undesirable in this design for two major reasons:

1. An electrolytic capacitor rated for 200-V would be physically large
2. Electrolytic capacitors are not desirable for MLPEs due to their short lifespans in wide temperature environments

To mitigate these issues, the input capacitance from the standard design was replaced with a ceramic type able to handle the voltage, and by nature, be more stable in higher temperature environments

2.2 Current Measurement

The primary goals of the current measurement feature in the TIDA-00640 are to minimize impact on the solar string and to provide reasonable accuracy. Because all of the modules in a solar string are typically placed in series, the current measurement must be able to support the entire string's output current. If the TIDA-00640 is intended to be placed at the input of an MLPE module and not the output, then only the single module's current needs to be accounted for because the MLPE will be passing the string current. Parallel module arrangements also result in a lower module current requirement. A current of 10 A was chosen as a maximum current capacity of the sense system; however, this could easily be resized to allow for more current or higher sensing accuracy.

A low-value current shunt resistor was chosen as the sensor in this TI Design to keep system complexity and cost to a minimum. This design uses a low-side sense element to reduce the need for high-voltage translation typical of a high-side element. Because the system is self-contained, this has no impact on the rest of the solar system beyond the minute power loss of the now series resistor.

Shunt resistors can provide their own complications; however, due to self-heating and power dissipation requirements. To this end, a limit of 100 mW was placed on the shunt. On a typical 300-W module, this results in a negligible power loss as shown in Equation 1:

$$\%\ \text{power loss from shunt} = \frac{\text{Shunt power dissipation}}{\text{Maximum module power}} \times 100 = \frac{0.100\ \text{W}}{300\ \text{W}} \times 100 = 0.03\% \quad (1)$$

The 1-mΩ shunt resistor is rated to 1% tolerance and 170 ppm. This shunt resistor was chosen with cost in mind. The ppm rating was lowered to a practical level for an MLPE, which operates in the upper range of 60ºC to 85ºC. To use a cost competitive shunt resistor, the tolerance was minimized at 1%. The shunt resistor's tolerance can be improved at the expense of component price or ppm rating. The shunt resistor's 1% tolerance equates to variances in board-to-board sensing accuracy, but it can be calibrated out.

A 1-mΩ shunt resistor at 10 A has a voltage output determined by Ohm's law as:

$$V_{OUT} = I \times R = 10\ A \times 0.001\ m\Omega = 0.01\ V \quad (2)$$

The TIDA-00640 uses the built-in ADC on the CC2538 for measurement. This is a 12-bit ADC with an input voltage range of 0 to V_{REF}. V_{REF} is selectable in software to be either an internal 1.15 V, or use an external reference attached to the VDD5 pin. To maintain a high dynamic range, the external V_{REF} was chosen for this TI Design and is attached to the board's VCC rail at 3.3 V. This provides an effective input range of 0 to 3.3 V. To ensure linearity and no saturation in the design, an upper limit of the voltage input was chose to be closer to 2.5 V.

The amplification circuit must then bring the 0.01 V of the shunt at 10 A to 3 V for the ADC. This is a normal gain of 300. To provide some additional overhead, a gain of only 260 will be used. This is achieved with a simple non-inverting amplifier configured with a 1.15-kΩ and 300-kΩ resistor in the feedback network. With this configuration, the final ADC input voltage at 10 A would be:

$$V_{IN} = 10\ A \times 0.001\ \Omega \times 261 = 2.6\ V \quad (3)$$

This input voltage can be correlated with V_{REF}, and the maximum ADC value (which is equivalent to V_{REF}) to determine the usable ADC range, and what the expected granularity is to validate that the design will be sufficient.

$$\frac{2^{12}}{3.3} = \frac{x}{2.6} \rightarrow x = 3227 \quad (4)$$

The value of 3227 is about 80% the full range of the ADC, as well as approximately what is expected at a full 10-A input. This also correlates to approximately 3 mA per ADC count, which is sufficient granularity for this TI Design, and well below the error expected to be injected from other sources.

In this simple implementation of a shunt-based current sense solution, there are several potential sources of error. The primary source is the potential for drift and offset in the amplifier. The specifications of the operation amplifier could be narrowed at the expense of system cost using a higher precision device like the OPA333 or a dedicated shunt amplifier such as the INA216.

The second primary source of error is the passive device tolerances. 1% devices were used across the system, which could lead to stacking of error and contribute to board to board variances of several percent. Tighter tolerance devices can be used to help increase board-to-board accuracy when using the same calibration constants.

2.3 Voltage Measurement

The TIDA-00640 uses a simple voltage divider and amplifier configuration to measure the module level voltage. A low upper limit was set to give the analog circuitry plenty of overhead in the case of higher than expected module voltage output. A divider of 50.8 was setup to bring the input of the amplifier at the full 90-V range down to 1.77 V. This 90-V range is specific to this board and can be reduced if the target system has a lower operating voltage, and more granularity is needed.

The voltage sensing divider feeds a simple buffer amplifier, which shares a package with the current sensing amplifier. As in the current measurement system, a V_{REF} of 3.3 will be used on the ADC of the CC2538. The slightly lower max input voltage limits the maximum ADC output to 2197; however, this still results in a granularity of 40 mV, or 0.0044% of full range, which is significantly beyond the requirements for this TI Design.

In order to minimize the power loss in the divider, high values resistors were used. A total drop of 510 kΩ results in only 177 µA of current draw from the module. Resistors with reasonably low temperature coefficient of 100 ppm and 1% tolerance were chosen to keep board-to-board variance and temperature drift low without sacrificing cost tolerance. Tighter specifications could be used for this analog front-end if required.

Two resistors were used on the high-voltage side of the divider to distribute the 90 V across multiple elements. If one of the resistors did happen to fail into a short state, the second resistors will be able to act as a failsafe to prevent the entire MPLE system from potentially failing from too much voltage being applied to the sensing circuitry.

2.4 Wireless Front End

One of the more complex portions of this design lies in the 2.4-GHz wireless front-end. These systems can be difficult to design and layout due to the complexities of RF signal transmission and reception. A robust filter network is typically required to ensure quality operation with minimal unintended radiation.

To keep total system complexity down, a PCB trace F-type antenna designed for 2.4-GHz systems was chosen. This design is specified to be 3.3 dB and only 25.7 × 7.5 mm. Thus, it is a compact, low-cost, and high-performance antenna. Find specifics on the antenna design itself and an implementation guide in the 2.4 GHz Inverted F Antenna design note[2].

The F antenna is a 50-Ω load to the CC2538 and must use a matching filter network. A typical filter network is shown in Figure 5. The filter network is nine discrete components, each of which must be chosen specifically and laid out on the PCB correctly.

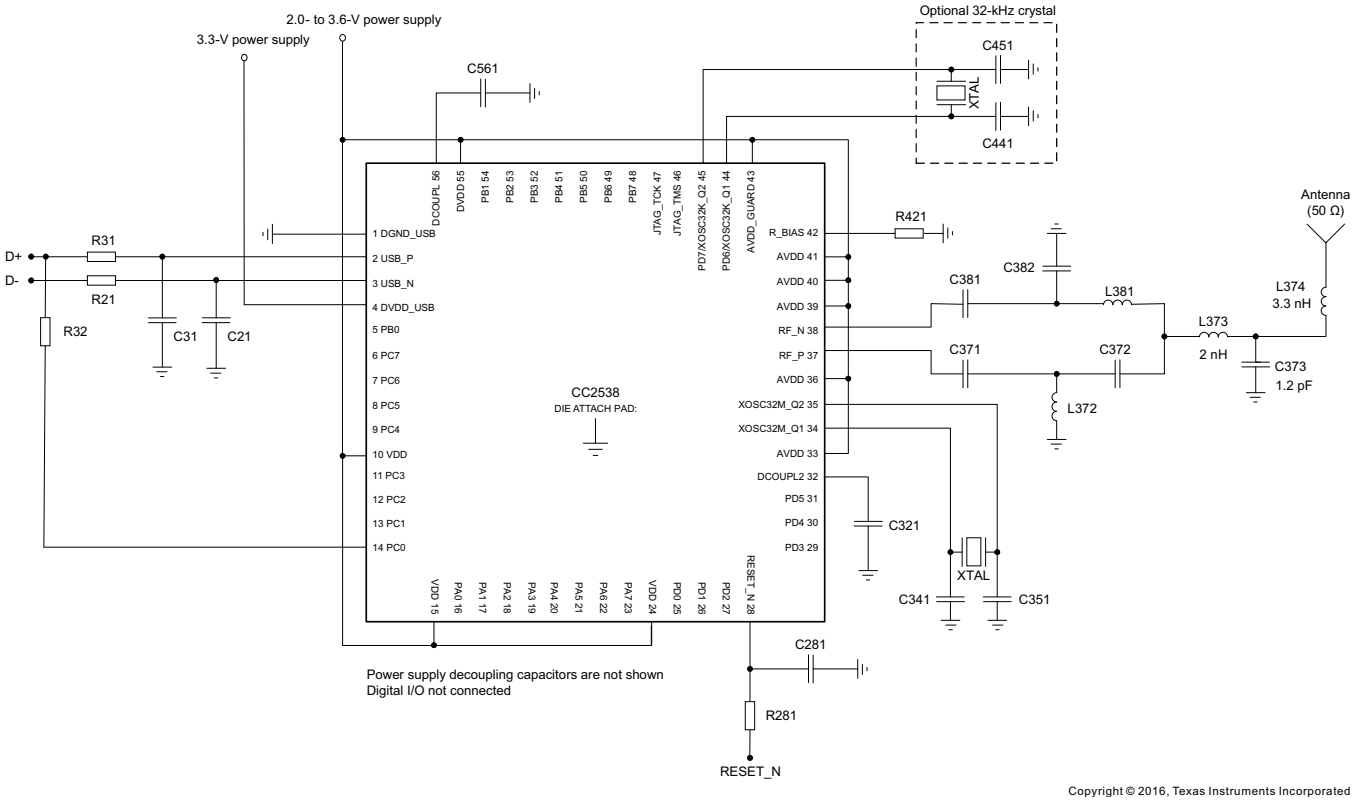

Figure 5. CC2538 Application Circuit

Murata Electronics has specifically designed an integrated balun, which replaces this entire filter network for the TI CC253x family of devices. This balun greatly simplifies the RF front end by reducing required board space, eliminating several components from the design, and helps to reduce any possible design errors. The balun also has integrated filter components to reduce unintentional harmonic radiation.

The final schematic of the RF front end is shown in Figure 6. The additional components on the output of the filter were used as placeholders for potential balancing needed in the design, but were not changed. The design operates as is with C14 and C15 being DNP, and R2 as a 0-Ω shunt.

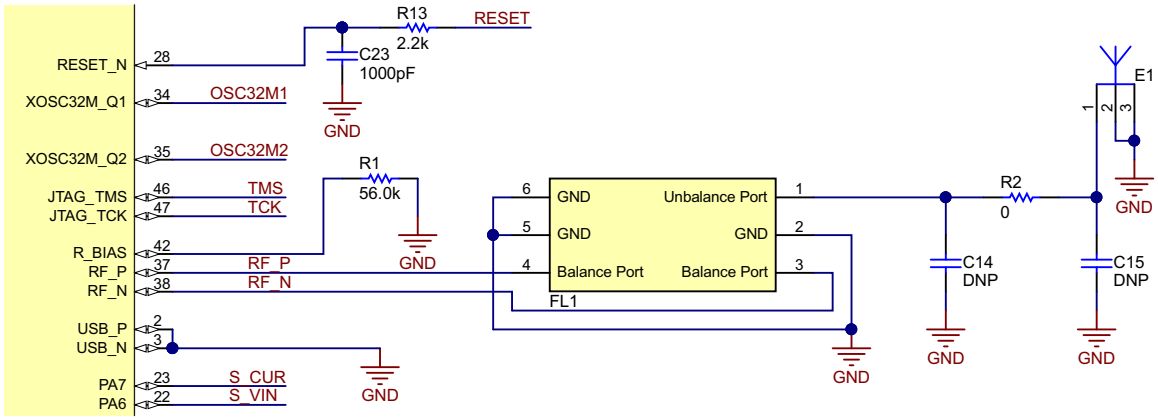

Figure 6. TIDA-00640 RF Front End

Additional information regarding the usage of the Murata balun, including design practices, guidelines, and measured performance characteristics is available in the device's application note[3].

2.5 Wireless Protocol

The TI CC2538 is a full SoC with an integrated IEEE 802.15.4 wireless radio. As such, the protocol support comes from the software stack chosen by the end user. At the time of publication, there are three major stacks fully supported on the platform: ZigBee PRO/2.0, ZigBee 3.0, and Contiki. The first two are developed by TI and can be certified by the ZigBee foundation, and the third is an open source 6LowPan wireless operating system.

ZigBee technology is supported by the ZigBee Alliance to ensure interoperability between various hardware and stacks from different manufacturers. The technology is designed to be a simpler and less expensive alternative to other wireless protocols on the market. ZigBee also enables sleepy devices for low power consumption while still having transmission distances from 10 to 100 meters. Additional network size can be achieved by implementing a mesh network. The mesh topology lends itself well to a solar module instillation because a large geographic area can be covered without the need for a centralized router, to which all end nodes would need to connect.

A typical mesh network is made of a single coordinator device, and then many routers and end devices. The data transmitted from one device will intelligently propagate through the network until it reaches its destination; typically, an edge router capable of translating the ZigBee data to a higher throughput interface such as Ethernet or Wi-Fi®. An example of a ZigBee mesh can be seen in Figure 7.

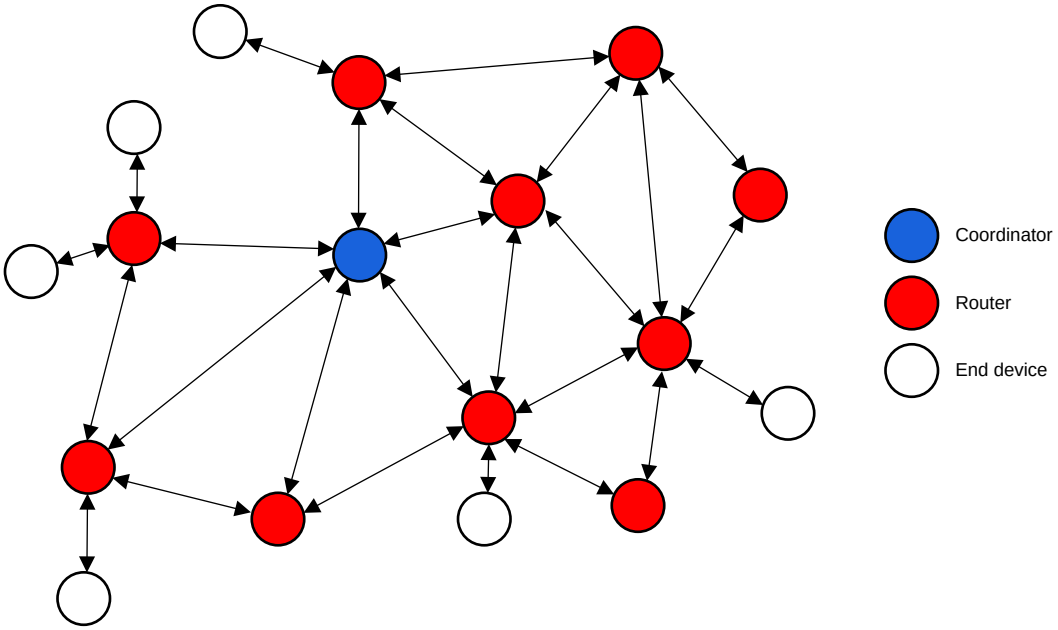

Figure 7. Mesh Network Layout

The CC2538 supports the ZigBee 2.0 specification through the Z-Stack software. This stack supports full IPv6, 128-bit security keys, and over 400 simultaneous nodes on the network. ZigBee 2.0 is divided into several application specific branches depending on the specific end device use case, including home automation, lighting, and smart energy. Additional information regarding Z-Stack and the ZigBee 2.0 implementation can be found on the software product page (http://www.ti.com/tool/z-stack). However, with the latest release, it is recommended to use ZigBee 3.0, which is backwards compatible with the 2.0 specification.

ZigBee 3.0 is an evolution of the ZigBee 2.0 specification that does away with the application layer specific protocols and moves to a single standard. This updated protocol is supported through the latest 3.0 release of TI Z-Stack and includes several key features beyond the profile unification including improved security features, seamless low power connection states, and full backwards compatibility with the older specifications. The latest version of Z-Stack is available at http://www.ti.com/tool/z-stack.

A third option is Contiki, which is an open source operating system for internet of things devices. It supports full IPv6 mesh, along with 6lowpan, RPL, and CoAP—all within a very small memory footprint. Additional information regarding Contiki as a whole is available from the project website (http://www.contiki-os.org/) and the TI implementation from the TI wiki: www.ti.com/contiki-6lowpan-wiki.

2.6 Temperature Sensor

The temperature sensing functionality of the TIDA-00649 is derivative of the internal analog temperature sensor in the CC2538 rather than using a discrete sensor. This internal sensor is specified to be accurate to ±10°C with no calibration or ±5°C with just a single-point calibration, which could easily be done at programing time during production.

The typical use case of a temperature sensor in a solar application is to derate power electronics in the event of the system crossing an over temp threshold. For that application, a more accurate remote sensor would be more applicable. With the built-in sensor on the CC2538, the design is able to self-monitor system level temperature at the module level rather than at the power conversion electronics. This data can then be used as part of a larger system level performance monitoring system.

Solar module efficiency is negatively related to module temperature or as the temperature drops the efficiency increases. Solar modules are general specified at 25°C. As the temperature increases above this point, the output current will rise, but the voltage output will drop faster, resulting in a decreased power output. As the temperature drops below 25°C, the inverse occurs. In extreme situations, the module could operate at up to 140% of the rated normal output.

Keeping track of the temperature can provide significant additional information regarding how a module is expected to perform versus how it is actually performing. This data helps end users understand how the array is aging and know if there are any potential problems that need to be remedied to maintain full output performance. For this generic metric, the guaranteed ±5°C of the internal CC2538 temperature is determined to be sufficient. If a tighter specification for system temperature monitoring is required, TI's array of pre-calibrated silicon based sensors enable an easy upgrade path.

3 Getting Started Hardware

3.1 Hardware

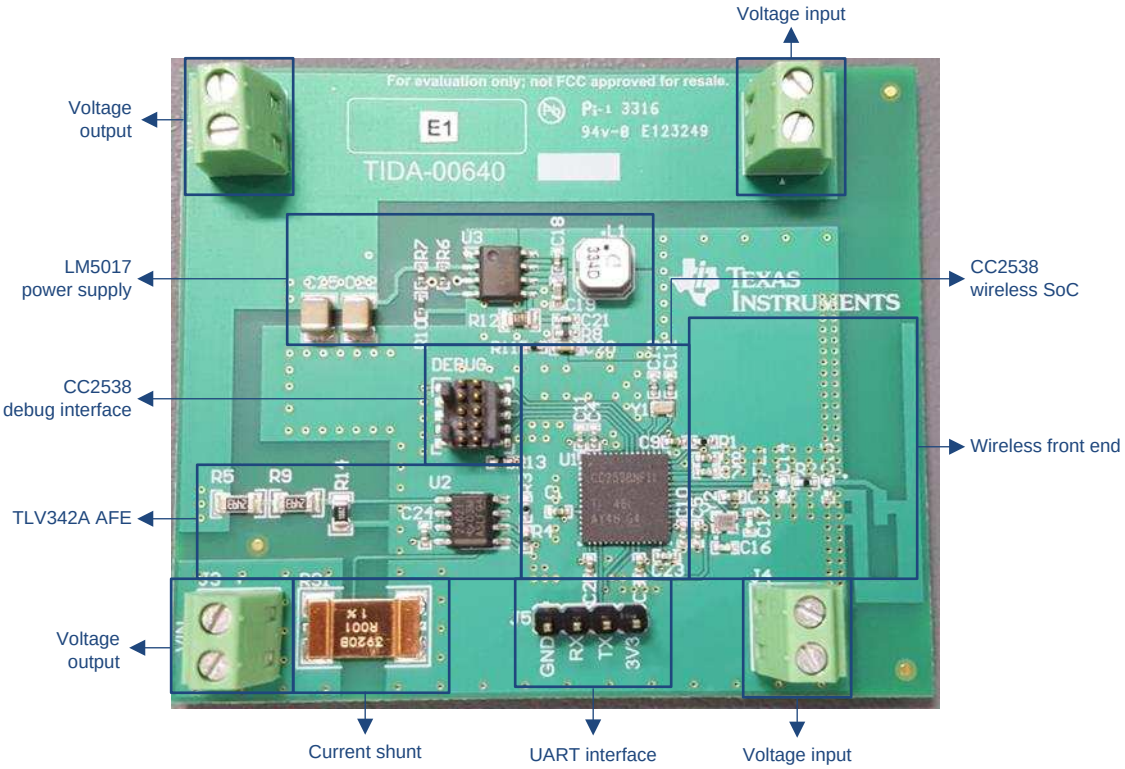

Figure 8. Hardware Overview

3.2 Test Setup

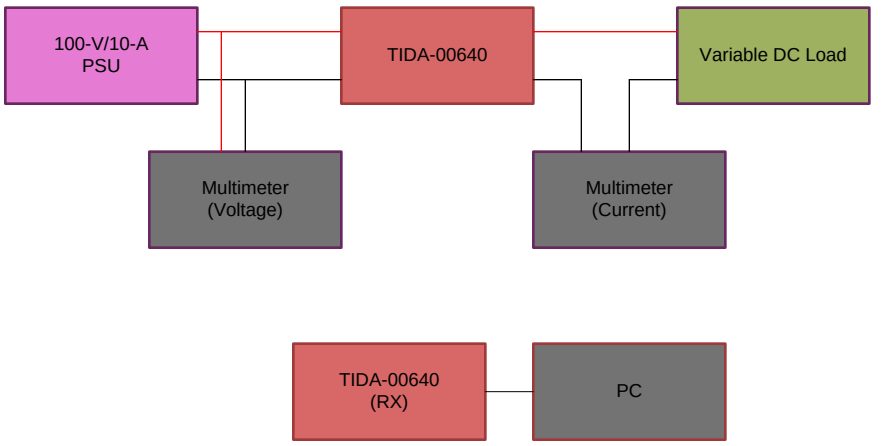

Figure 9. Current and Voltage Accuracy Test Setup

To fully test the design characteristics of the TIDA-00640, a power supply, DC load, and several calibrated meters were used. Because the design will be exposed to non-isolated high voltages, the RF capability was used to transmit raw ADC readings from both current and voltage channels to a receive device connected to a PC. The receive device was connected through J5 using a simple UART to USB serial bridge and read to a terminal window at 115200 baud.

The wireless stack used here is Contiki because it provided a simple interface, but has no bearing on the measurement accuracy. A custom sensor was designed based on the example Contiki application, which provides the raw sample data to the application layer. This sensor uses AVDD5 as the voltage reference and has a decimation rate of 512 to achieve the full 12-bit ENOB of the CC2538's onboard ADC. The same measurement scheme could easily be implemented in the other supported stacks. This 12-bit range was also scaled by eight by the Contiki stack to make some of the data structures more homogeneous across various libraries.

The variable DC load used is Kikusui PLZ15W, which is capable of 120-V DC, 10 A, and 150 W. Because it is not capable of sinking the full 1000 W that the board could measure, the voltage and current measurements need to be performed independently.

Two multimeters were used to enable simultaneous measurement of both current and voltage, which simplifies the testing procedure. For the voltage measurement, a Keithley 2001 series meter was placed in parallel with the design. A 10-A capable multimeter is required for the current measurement, so an Agilent U3401A meter was used in series.

Due to the same full power limitations in the DC load, two power supplies were required to be used to generate the full range 90-V and 10-A test scenarios. For the voltage test, a Xantrex XTR 100-8.5 source was used and a Sorensen DLM 60-10 was used for the current.

The final test setup used in the TI lab is shown in Figure 9. The TIDA-00640 under test is placed inside an interlocked enclosure to prevent accidental contact with the high voltage in the system. TI ESH guidelines place the exposed voltage limit at 50-V DC, but this may be different at other test sites. Use caution and follow local regulations regarding high-voltage electronics.

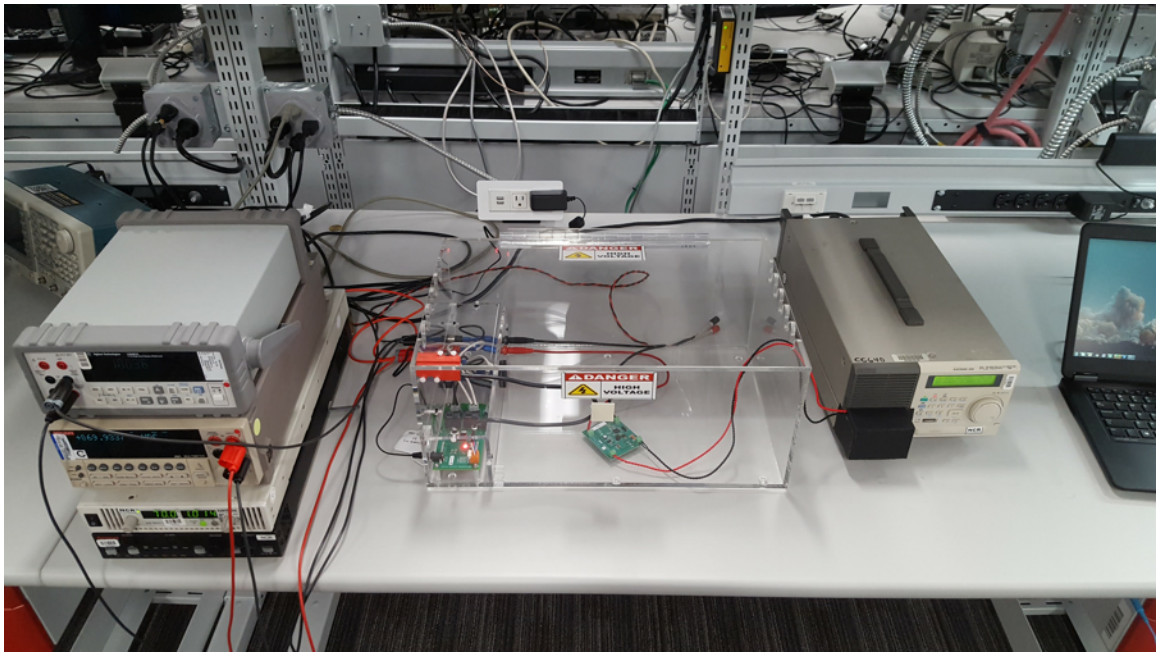

Figure 10. TIDA-00640 Test Setup

4 Testing and Results

4.1 Voltage Accuracy Testing

For voltage testing, the primary board input was used. This both powered the board under test and served as the measured value. As such, the lowest value able to be measured was approximately 6.3 V due to the input dropout voltage of the onboard power supply. The input voltage was measured to four significant figures, which is less than the 12-bit accuracy of the ADC, but accurate enough to ensure that the design falls within our designed accuracy specification and granularity.

A reference board was used to get a baseline of the relationship between applied voltage versus ADC measurement. Eighteen discrete samples were taken for this data set, each approximately 5 V apart in the 6- to 90-V range. For each voltage point, several ADC measurements were recorded to help determine how much deviation can be seen in the reading. Using a basic linear correlation, Equation 5 was developed to describe the relationship:

$$\text{Input voltage}(V) = 0.005 \times \text{ADC reading} + 0.2543$$

$$R^2 = 0.9999 \quad (5)$$

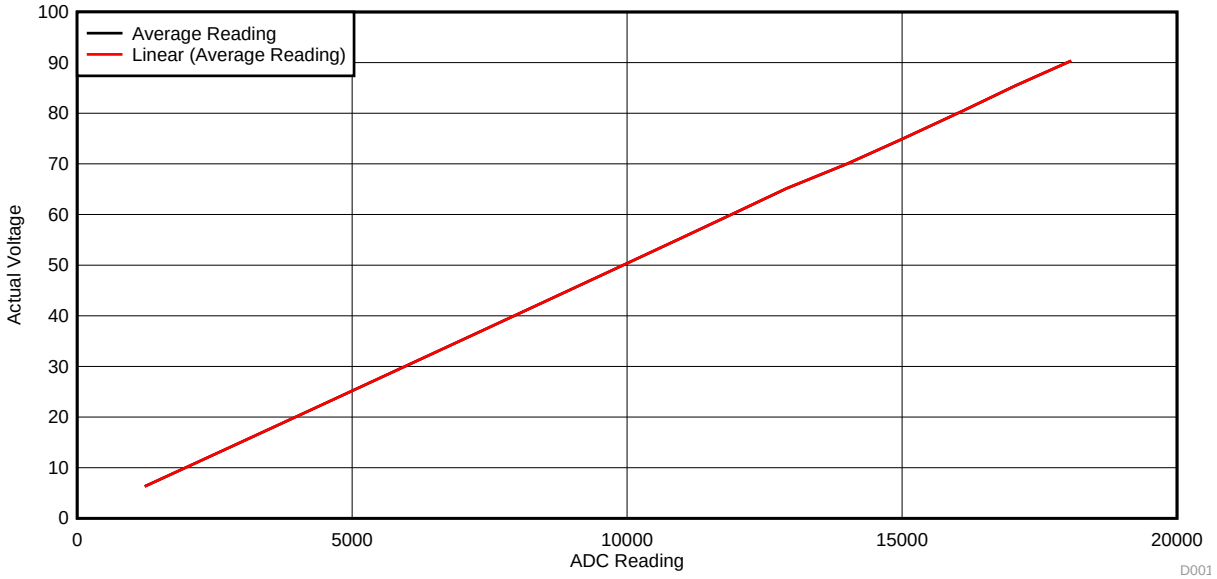

Figure 11. Voltage versus ADC Linearity

Using Equation 5, the expected voltages were back calculated using the actual ADC readings. This value is what the system would have measured as the input voltage from the solar module. These values were compared to the original measurement to determine the system induced error. This error over the voltage range is shown in Figure 12.

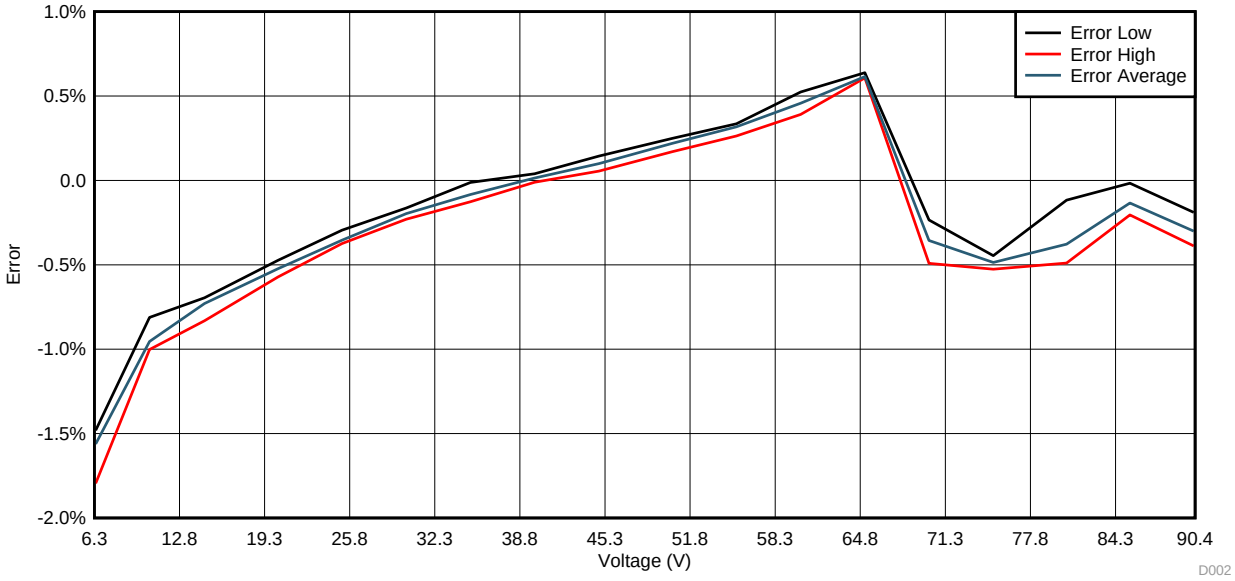

Figure 12. Calibrated Voltage Accuracy

These results show that on a single board with a custom fit calibration curve, all measurements are within 2% error. The relatively small gap between the high and low observed error shows excellent stability. It would additionally be possible to determine an even tighter curve for calibration, but this exercise is outside the expected scope of the design.

The calibrated results show excellent accuracy for a single board, but full multi-point calibration is often expensive and time consuming in practice. By using high precision components, the purpose of this TI Design is to ensure accuracy without individual board calibration. To validate this, the same test was performed across several other units of the TIDA-00640, where a known voltage was applied to the system (from 6 to 90 V at 5-V increments) and several associated ADC readings were measured.

Rather than use these measurements to create a fit, the relationship found on the first sample was used to back calculate to the applied voltage, and checked against the real measured value for accuracy. The accuracy results from one of these boards is shown in Figure 13.

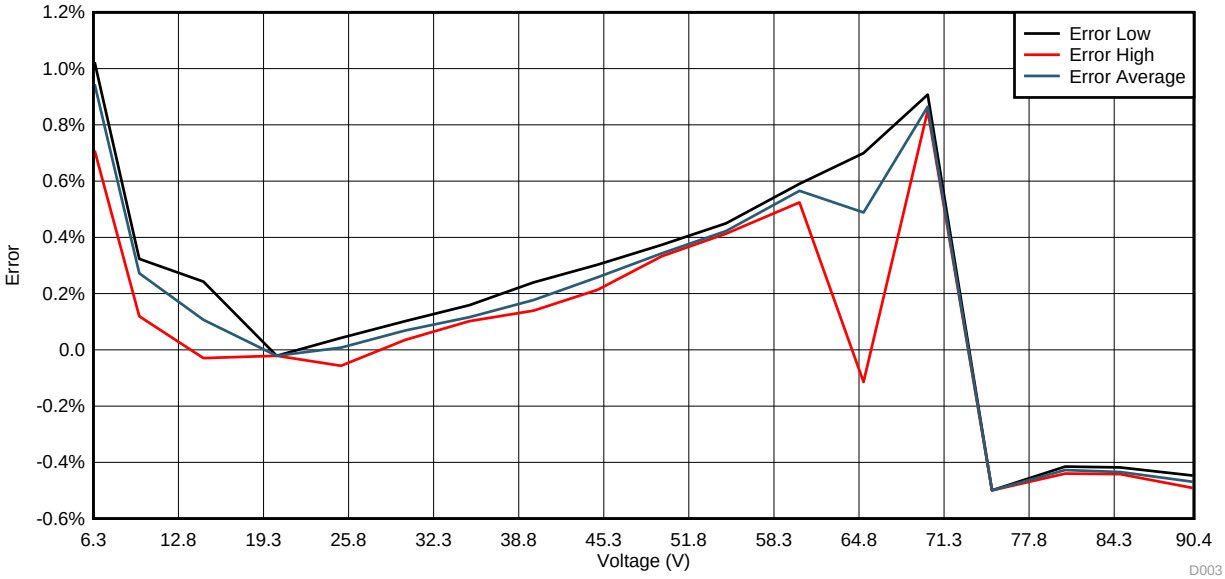

Figure 13. Calibrated Voltage Accuracy

This test method emulates a typical real world deployment situation where a generic relationship is developed to serve on many different boards in a production environment. The error for this deployment method is well within the error bounds of the system requirements.

4.2 Current Accuracy Testing

The current accuracy testing followed a similar procedure to the voltage testing. The board under test was powered through the primary input, and current was sourced from the board output using a variable programmable load. While under operation, the board was powered by the primary input as well, so a nominal voltage of 12 V was applied. This simulated a real world use scenario as close as possible with the whole system being under test. Full power could not be accurately tested due to limitations in the testing equipment, but because the measured signal is rather benign, there is little impact from the voltage measurement onto the current.

The reference board under test had a range of voltages applied, from 100 mA to 10 A, with steps of approximately 500 mA. For each current set point, several ADC readings were measured through the wireless link to determine stability. The current was measured with a multimeter with at least four digits of accuracy. The resultant data was used to extrapolate a linear fit to provide a mathematical relationship between the ADC reading and real current. For the reference board, this relationship was found to be:

$$\text{Input current}(\text{A}) = 0.0003695 \times \text{ADC reading} + 0.0458$$

$$R^2 = 0.9999 \quad (6)$$

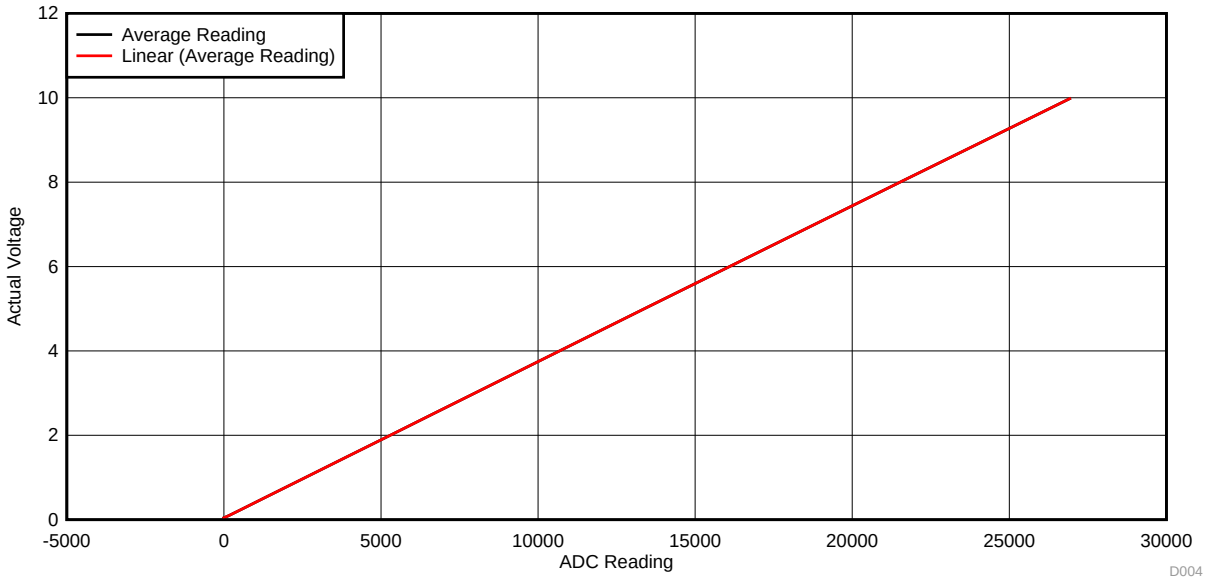

Figure 14. Current Linearity

This relationship was used to then back calculate from the ADC readings to the actual input current. This equates to how an actual solar system would report the system current. However, this would equate to a very tightly calibrated individual system. These were compared with the actual applied current to determine the accuracy of the measurement. The results of this can be seen in Figure 15.

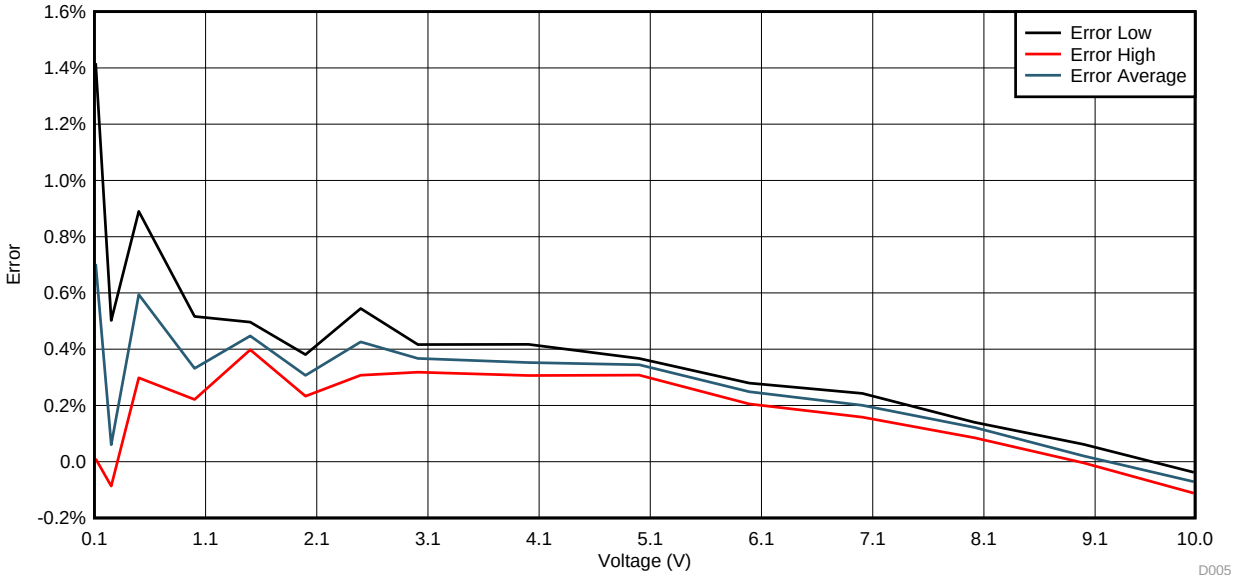

Figure 15. Calibrated Current Accuracy

The results show a total system accuracy with <2% error. As expected, the error increases at low current due to the offset voltages on the amplification stage, but is still well within the allowable range. As with the voltage measurement, the relationship developed on the reference board was applied to similar readings from a second board. The results from this can be seen in Figure 16.

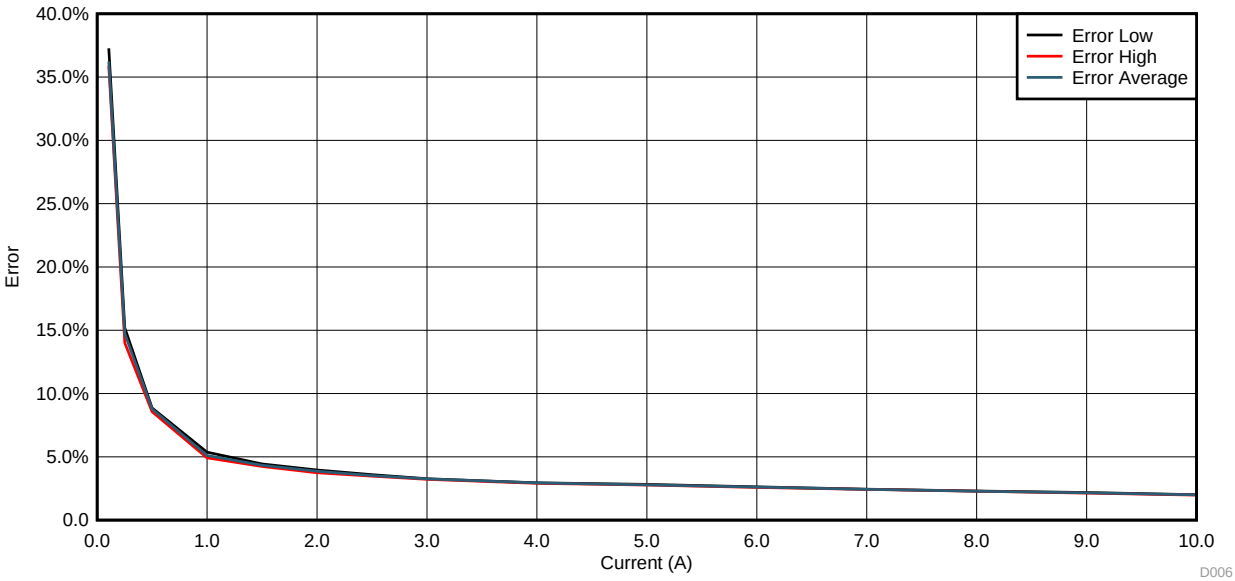

Figure 16. Uncalibrated Current Accuracy

In this case, the same levels found in the voltage test are not seen. The accuracy does not cross the 5% line until past 4 A, and then skyrockets at the low end. Looking back at the design, the major source of error is the offset voltage on the amplifier. Because of this, even with no current signal present there is an offset reading that is dominating the low-end measurements, and even impacting the high end where it is a lower percentage of the reading.

To solve this, the ADC reading at 0 A was taken and stored. This reading was then used as an offset to modify the readings for the rest of the current set points (while also taking into account the zero amp offset from the first board that is compensated for in the equation itself). Once the offset was applied, the new relationship is:

$$\text{Input current}(\text{A}) = 0.0003695 \times (\text{ADC Reading} + 90) + 0.0458 \quad (7)$$

This compensation factor can easily be self-determined by the system either during factory programing when it is powered externally, or during first startup. Using Equation 7, a new series of readings was back calculated to the original measurements, and compared to the multimeter readings to again determine the error. The results of this exercise are shown in Figure 17.

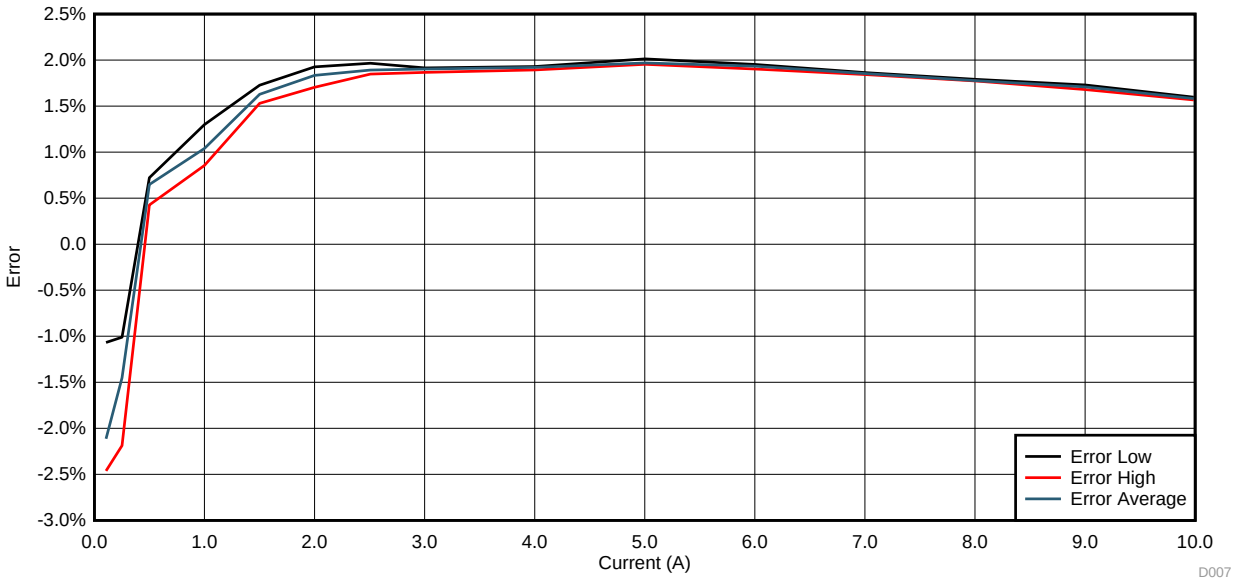

Figure 17. Compensated Uncalibrated Current Accuracy

The results of this compensated error curve show a significantly increased error across the entire test range. Observed here, the system is well below 5% and is within a 2% band for the entire system. These results fall well within the design expectations set forth.

5 Design Files

5.1 Schematics

To download the schematics, see the design files at TIDA-00640.

5.2 Bill of Materials

To download the bill of materials (BOM), see the design files at TIDA-00640.

5.3 Layout Prints

To download the layer plots, see the design files at TIDA-00640.

5.4 Altium Project

To download the Altium project files, see the design files at TIDA-00640.

5.5 Gerber Files

To download the Gerber files, see the design files at TIDA-00640.

5.6 Assembly Drawings

To download the assembly drawings, see the design files at TIDA-00640.

6 Related Documentation

1. Texas Instruments, *100-V, 600-mA Constant On-Time Synchronous Buck Regulator*, LM5017 Datasheet (SNVS783)
2. Texas Instruments, *2.4 GHz Inverted F Antenna*, Design Note DN0007 (SWRU120)
3. Texas Instruments, *Murata Balun for CC253x and CC254x LFB182G45BG2D280*, Application Note AN107 (SWRA380)

6.1 Trademarks

7 About the Author

BART BASILE is a systems architect in the Texas Instruments Grid Infrastructure Solutions Team, focusing on renewable energy and EV infrastructure. Bart works across multiple product families and technologies to leverage the best solutions possible for system level application design. Bart received his bachelors of science in electronic engineering from Texas A&M University.

IMPORTANT NOTICE FOR TI REFERENCE DESIGNS

Texas Instruments Incorporated ('TI") reference designs are solely intended to assist designers ("Designer(s)") who are developing systems that incorporate TI products. TI has not conducted any testing other than that specifically described in the published documentation for a particular reference design.

TI's provision of reference designs and any other technical, applications or design advice, quality characterization, reliability data or other information or services does not expand or otherwise alter TI's applicable published warranties or warranty disclaimers for TI products, and no additional obligations or liabilities arise from TI providing such reference designs or other items.

TI reserves the right to make corrections, enhancements, improvements and other changes to its reference designs and other items.

Designer understands and agrees that Designer remains responsible for using its independent analysis, evaluation and judgment in designing Designer's systems and products, and has full and exclusive responsibility to assure the safety of its products and compliance of its products (and of all TI products used in or for such Designer's products) with all applicable regulations, laws and other applicable requirements. Designer represents that, with respect to its applications, it has all the necessary expertise to create and implement safeguards that (1) anticipate dangerous consequences of failures, (2) monitor failures and their consequences, and (3) lessen the likelihood of failures that might cause harm and take appropriate actions. Designer agrees that prior to using or distributing any systems that include TI products, Designer will thoroughly test such systems and the functionality of such TI products as used in such systems. Designer may not use any TI products in life-critical medical equipment unless authorized officers of the parties have executed a special contract specifically governing such use. Life-critical medical equipment is medical equipment where failure of such equipment would cause serious bodily injury or death (e.g., life support, pacemakers, defibrillators, heart pumps, neurostimulators, and implantables). Such equipment includes, without limitation, all medical devices identified by the U.S. Food and Drug Administration as Class III devices and equivalent classifications outside the U.S.

Designers are authorized to use, copy and modify any individual TI reference design only in connection with the development of end products that include the TI product(s) identified in that reference design. HOWEVER, NO OTHER LICENSE, EXPRESS OR IMPLIED, BY ESTOPPEL OR OTHERWISE TO ANY OTHER TI INTELLECTUAL PROPERTY RIGHT, AND NO LICENSE TO ANY TECHNOLOGY OR INTELLECTUAL PROPERTY RIGHT OF TI OR ANY THIRD PARTY IS GRANTED HEREIN, including but not limited to any patent right, copyright, mask work right, or other intellectual property right relating to any combination, machine, or process in which TI products or services are used. Information published by TI regarding third-party products or services does not constitute a license to use such products or services, or a warranty or endorsement thereof. Use of the reference design or other items described above may require a license from a third party under the patents or other intellectual property of the third party, or a license from TI under the patents or other intellectual property of TI.

TI REFERENCE DESIGNS AND OTHER ITEMS DESCRIBED ABOVE ARE PROVIDED "AS IS" AND WITH ALL FAULTS. TI DISCLAIMS ALL OTHER WARRANTIES OR REPRESENTATIONS, EXPRESS OR IMPLIED, REGARDING THE REFERENCE DESIGNS OR USE OF THE REFERENCE DESIGNS, INCLUDING BUT NOT LIMITED TO ACCURACY OR COMPLETENESS, TITLE, ANY EPIDEMIC FAILURE WARRANTY AND ANY IMPLIED WARRANTIES OF MERCHANTABILITY, FITNESS FOR A PARTICULAR PURPOSE, AND NON-INFRINGEMENT OF ANY THIRD PARTY INTELLECTUAL PROPERTY RIGHTS.

TI SHALL NOT BE LIABLE FOR AND SHALL NOT DEFEND OR INDEMNIFY DESIGNERS AGAINST ANY CLAIM, INCLUDING BUT NOT LIMITED TO ANY INFRINGEMENT CLAIM THAT RELATES TO OR IS BASED ON ANY COMBINATION OF PRODUCTS AS DESCRIBED IN A TI REFERENCE DESIGN OR OTHERWISE. IN NO EVENT SHALL TI BE LIABLE FOR ANY ACTUAL, DIRECT, SPECIAL, COLLATERAL, INDIRECT, PUNITIVE, INCIDENTAL, CONSEQUENTIAL OR EXEMPLARY DAMAGES IN CONNECTION WITH OR ARISING OUT OF THE REFERENCE DESIGNS OR USE OF THE REFERENCE DESIGNS, AND REGARDLESS OF WHETHER TI HAS BEEN ADVISED OF THE POSSIBILITY OF SUCH DAMAGES.

TI's standard terms of sale for semiconductor products (http://www.ti.com/sc/docs/stdterms.htm) apply to the sale of packaged integrated circuit products. Additional terms may apply to the use or sale of other types of TI products and services.

Designer will fully indemnify TI and its representatives against any damages, costs, losses, and/or liabilities arising out of Designer's non-compliance with the terms and provisions of this Notice.

Mailing Address: Texas Instruments, Post Office Box 655303, Dallas, Texas 75265